Article

Laboratory and On-Road Evaluation of a GPF-Equipped Gasoline Vehicle

Ricardo Suarez-Bertoa [ID]**, Tero Lähde, Jelica Pavlovic, Victor Valverde, Michael Clairotte and Barouch Giechaskiel ***

European Commission, Joint Research Centre, 21027 Ispra, Italy

* Correspondence: barouch.giechaskiel@ec.europa.eu; Tel.: +39-0332-78-5312

check for updates

Abstract: The introduction of a solid particle number limit for vehicles with gasoline direct injection (GDI) engines resulted in a lot of research and improvements in this field in the last decade. The requirement to also fulfil the limit in the recently introduced real-driving emissions (RDE) regulation led to the introduction of gasoline particulate filters (GPFs) in European vehicle models. As the pre-standardisation research was based on engines, retrofitted vehicles and prototype vehicles, there is a need to better characterise the actual emissions of GPF-equipped GDI vehicles. In the present study we investigate one of the first mass production vehicles with GPF available in the European market. Regulated and non-regulated pollutants were measured over different test cycles and ambient temperatures (23 °C and −7 °C) in the laboratory and different on-road routes driven normally or dynamically and up to 1100 m altitude. The results showed that the vehicle respected all applicable limits. However, under certain conditions high emissions of some pollutants were measured (total hydrocarbons emissions at −7 °C, high CO during dynamic RDE tests and high NO_x emissions in one dynamic RDE test). The particle number emissions, even including those below 23 nm, were lower than 6×10^{10} particles/km under all laboratory test cycles and on-road routes, which are <10% of the current laboratory limit (6×10^{11} particles/km).

Keywords: real-driving emissions (RDE); on-road emissions; non-regulated pollutants; solid particle number emissions; sub-23 nm; low temperature −7 °C; worldwide harmonized light vehicles test procedure (WLTP); GPF; portable emissions measurement systems (PEMS)

1. Introduction

The introduction of vehicle emission standards in the European Union (EU) and the following tightening of the limits and more robust test procedures have been followed by the implementation of a series of exhaust aftertreatment systems. Emission limits for total hydrocarbons (THC), NO_x and CO for vehicles with spark ignition engines were followed by the wide introduction of the three-way catalyst (TWC). The introduction of emission limits on solid particle number (SPN) for vehicles with compression ignition engines was followed by the use of diesel particulate filters (DPFs) on all diesel vehicles [1]. Recently, following the introduction of SPN limits for gasoline direct injection (GDI) vehicles during the laboratory test cycle and the need to also comply with emissions performance requirements during the on-road real driving emission (RDE) test procedure, particle filters have become common also in these vehicles [2]. Similarly to their diesel counterpart (DPFs), these filtering systems are known as gasoline particle filters (GPFs).

The principle of operation of GPFs and DPFs is similar. However, there are profound differences in their operation environment. While the temperature of the exhaust of diesel vehicles is relatively low for soot oxidation and its removal from the filter (regeneration), in gasoline vehicles the temperature is often high enough for regeneration. However, in diesel vehicles the presence of NO_2 in the exhaust

gas can initiate DPF regeneration at lower temperatures, while for gasoline vehicles the three-way catalyst reduces NO_2 that could support oxidation at low temperatures [3]. In addition, while the level of O_2 in diesel exhaust is sufficient for regeneration at high exhaust temperature conditions, the concentration of O_2 in current gasoline cars with stoichiometric combustion is sufficient for soot oxidation only during fuel cut-offs. There are also substantial differences between gasoline and diesel exhaust in terms of particulate matter (PM) mass emissions, particle size and reactivity, and regeneration temperatures [4–6], which may lead to different mechanisms of filtration and regeneration. Moreover, as for diesel vehicles, even in the case of GDI vehicles, catalytic (i.e., catalyst-coated) filters might be needed to avoid uncontrolled soot combustion with local temperature excursions sufficiently high to damage the filter.

Recent studies showed that some modern cars (i.e., Euro 6) can have high emissions of regulated pollutants on the road, for example NO_x [7] and also CO and particle number, during dynamic driving [8,9]. Emissions of NO_2 as well as NO to NO_2 ratio are of environmental relevance as the increase in NO_2 to NO ratio in vehicle exhausts has been shown to affect urban atmospheric chemistry, both ozone (O_3) and secondary organic aerosol formation, and consequently worsen urban air quality. In fact, the European Environmental Agency (EEA) has recently reported that, following the decrease of the ratio of NO to NO_x emissions for diesel vehicles, which leads to less O_3 being consumed in the titration reaction with NO, O_3 concentrations near sources of traffic emissions have increased in several traffic stations [10]. For that reason, the NO_2 emissions and NO to NO_2 ratios of GPF-equipped vehicles need to be evaluated.

Non-regulated pollutants such as NH_3 are sometimes high in gasoline vehicles [11,12]. In gasoline cars, NH_3 is formed in the TWC via steam reforming from hydrocarbons [13] and/or via reaction of NO with molecular hydrogen (H_2) produced from a water-gas shift reaction between CO and water [13,14]. Moreover, it has been shown that vehicular NH_3 emissions depend on road grade, driving mode and vehicle age [11,15]. Emissions of formaldehyde (HCHO) and acetaldehyde (CH_3CHO), two pollutants whose measurement is included in the UNECE (United Nations Economic Commission for Europe) Global Technical Regulation (GTR) 15, are typically related to incomplete combustion and cold-start emissions before the TWC light-off. Formaldehyde is mainly produced from isoparaffins and alkyl aromatics [16]. Partial combustion of isoparaffins and alkyl aromatics results in increased formation of methyl and ethyl radicals, which can undergo further reactions to form formaldehyde. Acetaldehyde can be formed from alkyl aromatics. Acetaldehyde is also produced from the partial oxidation of ethanol, with straight-chain hydrocarbons also enhancing the formation of acetaldehyde by C2 hydrocarbons, such as ethylene and ethyl radicals [17]. The impact of GPFs on the emissions of gaseous pollutants, especially non-regulated ones, is limited [18]. Some recent studies that evaluated the performance of GPFs on retrofitted vehicles [18,19] indicated that they not only reduce particle number emissions from the gasoline vehicles but, if catalysed, could also reduce emissions of gaseous pollutants.

GPFs can be catalyst coated or not [19]. The primary benefit of bare GPF is that it can be designed as a stand-alone component without significant changes to the upstream TWC, which is already optimized to meet low tailpipe gas emissions. The absence of catalyst allows for the use of smaller pore size to achieve high filtration efficiency without a significant pressure drop penalty. Catalytic GPFs can be used within exhaust aftertreatment systems to control gaseous emissions, providing equivalent performance by replacing some or all of the catalyst volume, enabling more compact GPF designs. The addition of a catalytic GPF may further reduce pollutants and maintain performance over the lifetime. While most of the recent studies provide results for prototypes or retrofitted vehicles, often optimized to present the best possible filtration performance [2,19], in the present study we investigate one of the first vehicles with GPF available in the European market in mass production. This should provide a better understanding of the mechanisms of filtration and regeneration and overall performance presented by this relatively new technology under representative laboratory and on-road conditions. It should also be the basis for future more advanced catalytic GPFs.

In this study, different test cycles and conditions in the laboratory and on-road are considered, including different routes (even outside the RDE boundary conditions) covering a wide range of the engine map, engine cold and hot starts, and different ambient temperature (23 and −7 °C) and pressure conditions (up to 1100 m). Hence, a comprehensive study of the gaseous and particulate regulated and non-regulated emissions, namely NH_3, N_2O, HCHO, CH_3CHO, aromatic compounds (AHC) and solid particles below 23 nm from a GPF-equipped Euro 6b compliant gasoline vehicle is performed under a wide variety of real world conditions. The results are compared with some of the latest findings reported for gasoline vehicles.

2. Results and Discussion

2.1. Laboratory Emissions

Distance-specific emission of the regulated and non-regulated pollutants and CO_2 obtained for the Euro 6b compliant GPF-equipped GDI vehicle over the New European Driving Cycle (NEDC) at 25 °C and the Worldwide Harmonized Light Vehicles Test Procedure (WLTP) at 23 °C and −7 °C are summarized in Table 1.

Table 1. Average emission (mass/distance units) for the regulated and non-regulated gases and CO_2 and particulates over the New European Driving Cycle (NEDC) and the Worldwide Harmonised Light Vehicles Test Procedure (WLTP) at 23 °C and −7 °C. Errors refer to the difference from max and min values of two tests performed. SPN_{23} and SPN_{10} stands for solid particle number emissions above 23 nm and 10 nm, respectively.

Pollutant	Unit	Instrument	Euro 6b Limits (NEDC Based)	NEDC 25 °C	WLTP 23 °C	WLTP −7 °C
CO_2	g/km	NDIR	(132) [1]	137 ± 3	153 ± 3	169 ± 2
CO	mg/km	NDIR	1000	110 ± 2	178 ± 32	706 ± 102
THC	mg/km	FID	100	27 ± 4	17 ± 8	129 ± 12
NMHC	mg/km	FID	68	24 ± 10	14 ± 7	118 ± 13
CH_4	mg/km	FID			3 ± 0	11 ± 1
NO_x	mg/km	CLD	60	25 ± 2	30 ± 4	46 ± 2
NO_2	mg/km	CLD			15 ± 2	15 ± 2
NH_3	mg/km	FTIR			11 ± 2	27 ± 3
N_2O	mg/km	FTIR			2 ± 0	2 ± 1
HCHO	mg/km	FTIR			0.1 ± 0	0.2 ± 0
CH_3CHO	mg/km	FTIR			0.2 ± 0	0.8 ± 0.1
AHC	mg/km	FTIR			5 ± 3	42 ± 1
SPN_{23}	$\times 10^{10}$ p/km	CPC	60 [2]	2.5 ± 0.1	3.5 ± 0.1	4.5 ± 0.1
SPN_{10}	$\times 10^{10}$ p/km	CPC			4.8	7.1

[1] declared; [2] ten times higher limit may be applied. AHC = aromatic compounds; CH_3CHO = acetaldehyde; CLD = chemiluminescence detector; CPC = condensation particle counter; FID = flame ionization detector; FTIR = Fourier transform infrared spectrometer; HCHO = formaldehyde; NMHC = non-methane hydrocarbons; NDIR = non-dispersive infrared; SPN = solid particle number; THC = total hydrocarbons.

2.1.1. Cycles at 23–25 °C

The NEDC results respected the Euro 6b limits (Table 1). Emission of the regulated pollutants of the WLTP at 23 °C were well below the Euro 6 limits, even though this vehicle was type approved under the NEDC. Carbon monoxide (CO) emissions (178 mg/km) were comparable to what was reported in recent Euro 6 studies [7,8,20,21]. These studies present the widest emission source currently available for Euro 6b gasoline vehicles tested at 23 °C or −7 °C. CO emissions were also in agreement or lower with those reported for GPF-GDI vehicles and engines [22–24].

Emissions of total hydrocarbons (THC) were low (17 mg/km). These emissions were in agreement with those reported for a Euro 6b and China 6 GDI vehicles (not equipped with GPF) under the same conditions (i.e., WLTP at 23 °C) [8,20,21,25] as well as for various GPF-GDI vehicles and engines [23,24,26].

Roughly 80% (14 mg/km) of the THC emissions were non-methane hydrocarbons (NMHC), of which 36% (5 mg/km) corresponded to aromatic compounds (AHC). This suggests a similar efficiency of the system used by the tested vehicle (TWC + GPF) when reducing NMHC compared to similar vehicles equipped just with a TWC [20]. The NMHC results are in good agreement with others [23] for NMHC and additionally with a study [27] that reported no decrease on the emissions of NMHC or aromatic compounds from a series of retrofitted GDI vehicles.

NO_x emissions (30 mg/km) were comparable to those reported in the literature [22,23,26]. Interestingly, while up to now NO_2 from stoichiometric gasoline vehicles have been reported to be negligible, or below the limit of detection of the used instruments [20], NO_2 emissions from the tested GPF-equipped vehicle represented approximately 50% (15 mg/km) of the NO_x emissions. This suggests that passive soot regeneration of GPF is, in this vehicle, boosted with NO_2 formed in TWC at lean, fuel-cut conditions, similar to passive regeneration of DPF [28]. It should be stressed, however, that the absolute levels of NO_x for the vehicle were quite low, only half of the applicable limit (60 mg/km for NO_x).

Ammonia (NH_3) emissions (11 mg/km) from the GPF-equipped GDI vehicle studied were 2 times lower than what has been reported for other Euro 6b GDIs tested at 23 °C [20,29,30] and comparable to what has been reported for a Euro 6b plug-in hybrid GDI (7 ± 1 mg/km) [31]. This suggests that this vehicle with this aftertreatment system do not diverge from the levels of NH_3 emissions currently reported for gasoline vehicles. NH_3 emissions from the GPF-equipped GDI were 1.6 to 10 times higher than those reported for a series of China 6 vehicles tested using the WLTP at 23 °C [25] and 2 times higher than what was reported by for a European Euro 6 GDI [21]. Other researchers who measured NH_3 emissions for a GDI vehicle before and after being retrofitted with a GPF did not observe a change in NH_3 emission rates [32].

N_2O emissions (2 mg/km) were 4 times higher than those reported for a Euro 6b GDI (0.5 mg/km) [21]. The emissions were slightly higher than those reported in previous studies for Euro 6b GDIs conventional [20] and plug-in hybrid [31] and also from a Euro 5b flex-fuel tested on the WLTP [33,34]. The N_2O emissions accounted for ~0.35% of the CO_2 equivalent grams (100 years global warming potential 265 CO_2 g eq/g) emitted by the vehicle. Moreover, the N_2O emissions were well below the China 6 emission standards (20 mg/km).

Emissions of formaldehyde (HCHO) (0.1 mg/km) and acetaldehyde (CH_3CHO) (0.2 mg/km) were comparable to those reported in previous studies for GDIs [21], flex-fuel vehicles [33,35] and conventional hybrid vehicles [36] tested on the WLTP at 23 °C. They were close to the detection limit of the measurement instrument (FTIR).

The solid particle number (SPN) emissions (3.5×10^{10} p/km) were <1% of the applicable limit for this vehicle (6×10^{12} p/km) or <10% of the current limit (6×10^{11} p/km), even when including particles below 23 nm.

2.1.2. Cycles at −7 °C

Emission substantially increased when the vehicle was tested at cold ambient temperature (−7 °C), compared to 23 °C (Table 1). This negative effect has been previously reported for Euro 5 and Euro 6 vehicles [7,20,37–39]. These studies (and the references therein) summarize that at lower ambient temperatures, the engine and catalyst take longer to warm up, which results in higher emissions. They indicate that at cold ambient temperatures rich combustion is commonly used in gasoline vehicles, to avoid misfires, resulting in incomplete fuel combustion, hence, higher CO and hydrocarbon emissions. Moreover, since the TWC requires a certain temperature (typically above 300 °C) to efficiently reduce engine out emissions, these emissions are significantly higher until the catalytic converter reaches operational working conditions [40,41].

THC and NMHC were one order of magnitude higher at −7 °C compared to 23 °C (129 mg/km and 118 mg/km, respectively). CO (706 mg/km) and NO_x (46 mg/km) increased 4 times and 50% respectively under these conditions. Although emissions increased at cold temperatures, they were

close (THC) or below the limits required at 23 °C. At cold temperature, emissions were also comparable to those previously reported for Euro 6b gasoline vehicles without GPF [8,20,38], with the exception of CO which were 2 times lower than those reported by others [38]. It should be noted that currently only THC and CO emissions are regulated at −7 °C (UNECE Regulation 83). The limits, 15,000 mg/km for CO and 1800 mg/km for THC, must be met during the urban part of the NEDC.

Regarding the non-regulated pollutants, NH_3 emissions (27 mg/km) were 2.5 times higher at −7 °C than at 23 °C and N_2O (2 mg/km) and NO_2 (15 mg/km) did not vary. Emissions of NH_3 and N_2O were comparable to those reported in a series of studies that investigated emissions of non-regulated pollutants from conventional gasoline, hybrid and plug-in hybrid vehicles at cold ambient temperatures [20,31,36]. NO_2 was slightly higher than what was reported for Euro 6b gasoline vehicles, which were below the limit of detection.

HCHO (0.2 mg/km) and CH_3CHO (0.8 mg/km) emissions were slightly higher than at 23 °C, but still very low. The increase is in line with what was reported in previous studies [11,30]. However, HCHO emissions were lower than those reported for spark ignition vehicles (conventional and hybrids) tested under similar conditions (0.4–1.8 mg/km) [11,33,35].

AHC emissions (42 mg/km) increased by a factor of 8.4, still representing 36% of the NMHC emissions.

The SPN emissions increased 30–55% but remained at approximately 1% of the applicable limit of this vehicle or 10% of the current limit.

2.2. Modified Cycles

Figure 1 summarises the regulated gaseous pollutants emissions for the driving cycles and their variations. The measured CO_2 at the cold NEDC (a test that replicates the official type-approval conditions) was 3.5% higher than the declared value [42].
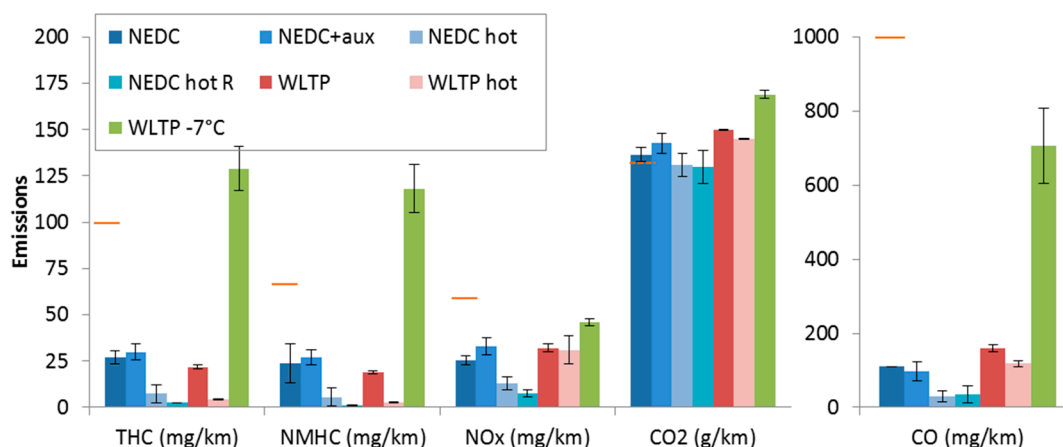
Figure 1. Gaseous emissions for various test cycles. Solid orange lines show the Euro 6b limits (for Euro 6b applicable over the NEDC). The orange dotted line shows the declared CO_2 value.

In general, most of the results were below the applicable Euro 6b emission limits and the differences between the modified and the standard cycles are small or within the tests variability. The exceptions are the −7 °C WLTP tests that were discussed previously.

Figure 2 illustrates the SPN emissions for various test cycles. The measured vehicle SPN were below 1×10^{11} p/km, well below the SPN_{23}-limit of 6×10^{12} p/km for Euro 6b (current Euro 6 limit for GDIs is 6×10^{11} p/km). The highest SPN_{23} and SPN_{10} emissions were measured for WLTP −7 °C, where the emissions were still only 1% of the Euro 6b SPN-limit or 10% of the 6×10^{11} p/km current limit. This point is important, because other non-GPF equipped GDIs with SPN levels well below 6×10^{11} p/km exceed the 6×10^{11} p/km limit at low temperatures or aggressive driving [21,22].

The WLTP SPN emissions were higher than the NEDC emissions, in agreement with others [22], but the emission levels were too low to discuss significant differences. The measured SPN emissions are in line with some of the results found in the literature. For example, the SPN_{23} emissions of a GPF-retrofitted Euro 5 GDI vehicle over ambient temperature NEDC were below the limit [43]. Similar results were shown for other retrofitted GPF GDI-vehicles over NEDC [22,26,44] and over WLTP [22]. On the other hand, others have shown that the SPN emissions of GPF-equipped vehicles are close to the limit [24,32]. Long term studies showed that the filtration efficiency of GPFs depends on the accumulated soot, but also ash; thus, it improves with mileage accumulation [23,45]. The vehicle of our study had been driven close to 5000 km when the laboratory tests started.

The cold start emissions were higher than the hot start SPN_{23} and SPN_{10} emissions for both NEDC and WLTP, around 80% and 70% respectively (compare NEDC vs. NEDC hot and WLTP vs. WLTP hot). The modified cycle SPN emissions were only slightly higher than the standard ones. The NEDC with the auxiliaries had 16% and 19% higher SPN_{23} and SPN_{10} emissions compared to the cold start NEDC. The repeated hot NEDC without turning off the engine (NEDC hot R) had 11% and 19% higher SPN_{23} and SPN_{10} emissions than the hot start NEDC.

The repeatability of the measurements, calculated as the difference of the maximum value from the mean, was better than 5% for both 23 nm and 10 nm measurements.

The excess of SPN_{10} in comparison to SPN_{23} was slightly higher for NEDC than that determined for the WLTP. Over the NEDCs, the excess emissions were in the range 31–48%, while for WLTPs, they were in the range 26–28% (50% for the −7 °C test), in agreement with others [46–50]. In the literature, a wide range of sub-23 nm fractions are reported: from negligible [43] to 9 times more for the more aggressive US06 cycle. However, it was concluded that the 9 times higher sub-23 nm particles were formed downstream of the GPF due to the high exhaust gas temperatures; results by others [51] support this conclusion.
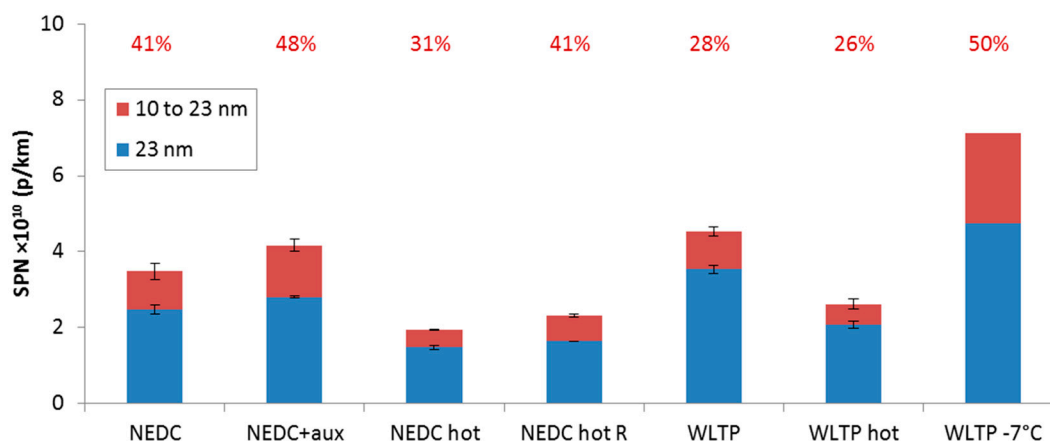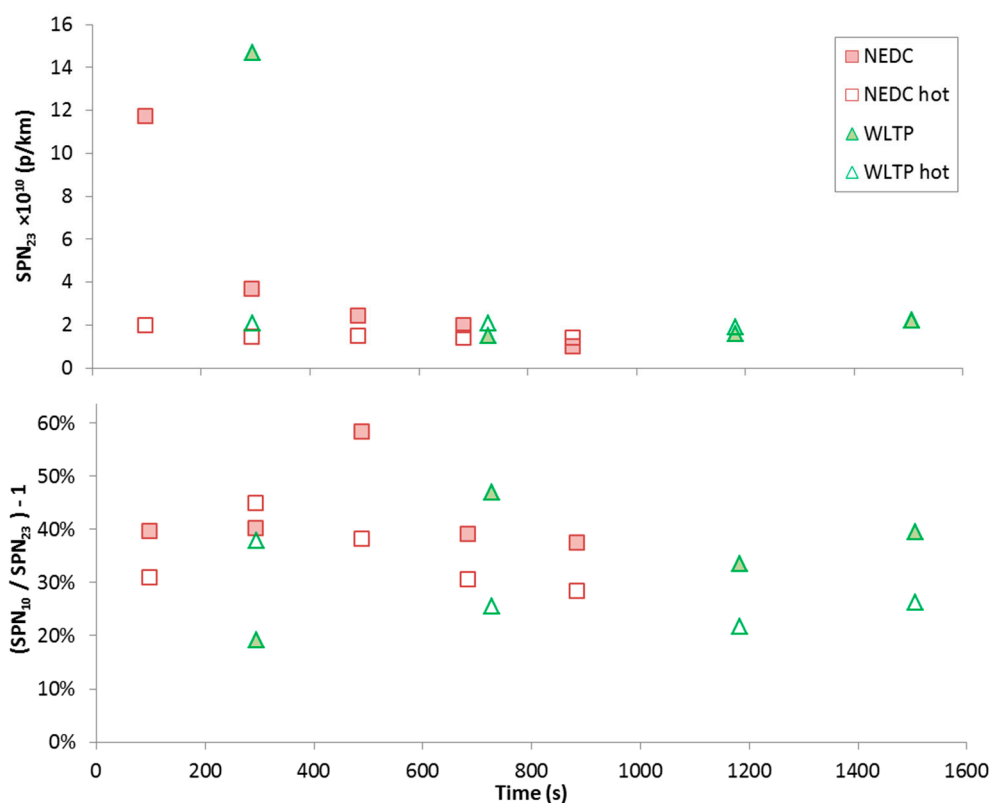

Figure 2. Solid particle number (SPN) emissions for various test cycles. The percentages give the excess of particles below 23 nm. The SPN limit is 6×10^{11} p/km and a ten times higher limit may be applied for the specific vehicle.

The differences between cold and hot start cycles were further examined. The emissions were calculated for each phase of the NEDC (ECE-15 × 4, EUDC) and WLTP (Low, Medium, High, Extra High) and were plotted in function of the time (the midpoint of each phase was taken) (Figure 3, upper panel). For the hot start NEDC and WLTP the SPN_{23} emissions were at the same levels for all phases and each phase contributed equally (open symbols). For the cold start NEDC and WLTP the emissions were the highest at the 1st phase, contributing 59% and 74% respectively of the total cycle emissions (solid symbols). Then, the emissions decreased and reach the hot cycles emissions. The other modified cycles had similar behaviour depending on whether they were with cold or hot start (no Figure is shown).

In general, the majority of the emissions originated from the cold start, in agreement with others [8,32] who showed that cold-start emissions were 60–70% higher for Euro 6b GDI vehicles without GPF. Higher differences (150%) were found with a GDI-GPF vehicle at the US06 cycle [46]. However, the GPF filtration efficiency depends on the driving history of the vehicle and condition of the filter [44,46].

The sub-23 nm excess particles (Figure 3, lower panel) varied in the 20–60% range. The 1st phase of the cold WLTP was at the low end indicating larger particles during cold start, which is in agreement with the literature for GDI vehicles [52]. However, the percentages have high uncertainty due to the low particle number concentrations.

Figure 3. Solid particle number (SPN) emissions for various test cycles (upper panel) and percentages of excess of particles below 23 nm (lower panel).

2.3. On-Road Emissions

The emissions of CO, NO_2, NO_x, CO_2 and SPN_{23} obtained for the vehicle studied along four different routes (RDE-1, RDE-2, City-Motor, Hill) and two different driving styles (normal, dynamic) are summarized in Table 2. A "D" in the test identification indicates that the driving style was dynamic.

Table 2. Emissions for the various routes.

	RDE-1	RDE-2	RDE-1-D	RDE-1-D *	RDE-2-D	City-Motor	Hill
CO_2 (g/km)	173	170	193	178	189	158	182
CO (mg/km)	189	133	3973	2409	3065	181	149
NO_x (mg/km)	24	15	23	205	25	16	18
NO_2 (mg/km)	2	1	2	12	2	2	3
SPN_{23} ($\times 10^{10}$ p/km)	2.0	1.7	4.9	2.3	4.1	1.3	1.4

* Asterisk indicates a repeat with a different driver.

The measured CO_2 emissions of the RDE compliant routes were approximately 30% higher than the declared NEDC value and 12% higher than the WLTP measured value [42]. The other pollutants (CO, NO_x, SPN) were in good agreement with the laboratory results. Yet, the on-road NO_2 to NO_x ratio was 10% while in the laboratory it was 50%. The emissions of regulated pollutants on the Hilly and the City-Motorway routes were in line with the RDE compliant routes. The CO_2 emissions were 9% lower at the City Motorway route and 6% higher at the Hilly route than at the RDE compliant routes. It should be noted that driving dynamics, ambient temperature, road grade, traffic, and use of auxiliaries influence the final CO_2 values and that no detailed analysis was performed to explain route-to-route differences in CO_2 emissions as it is beyond the scope of the research.

During dynamic driving tests, NO_x emissions remained at the same levels. The CO emissions (3000–4000 mg/km) were up to 20 times higher than during the RDE-compliant tests, originating from the accelerations (Figure 4). The complete cycles are plotted in Figure A2 (Appendix A).
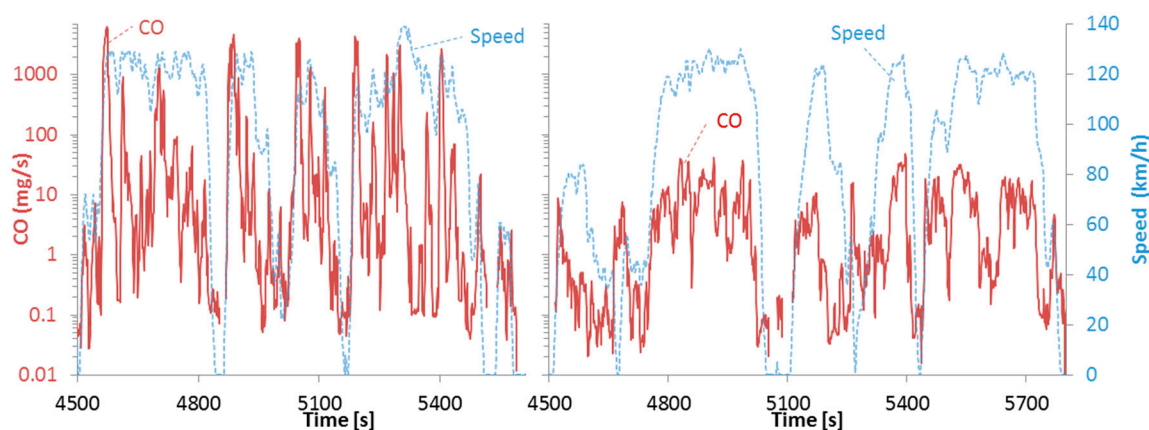
Figure 4. Carbon monoxide (CO) emissions for the motorway parts of dynamic RDE-1 (RDE-1-D) (left panel) and (normal) RDE-1 (right panel).

The SPN_{23} emissions were two times higher (up to 4×10^{10} p/km) than during the other on-road tests but still one order of magnitude below the 6×10^{11} p/km Euro 6d laboratory limit (not even considering the 1.5 conformity factor for SPN) confirming the effectiveness of the GPF technology. The SPN emissions followed the accelerations and engine speed (Figure 5). There were no clear indications of spikes during decelerations even at the motorway parts (Figure 5) where the exhaust gas temperature is relatively high.
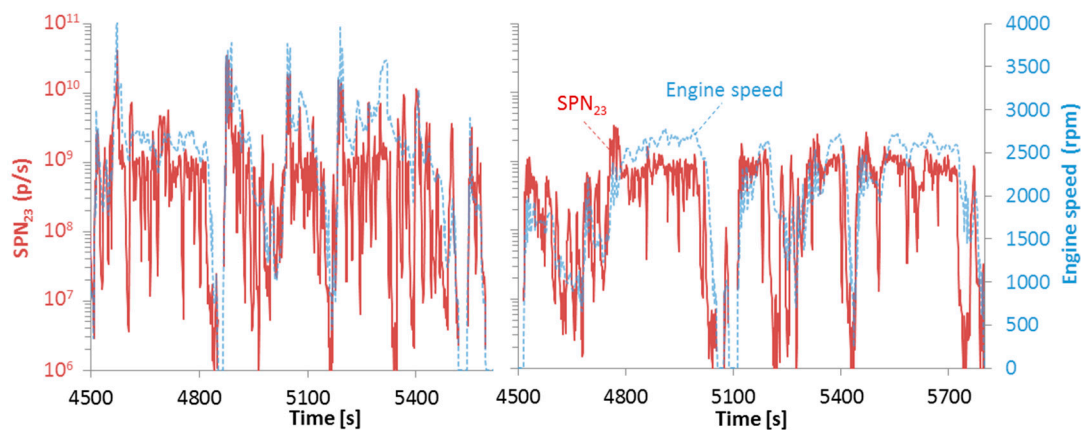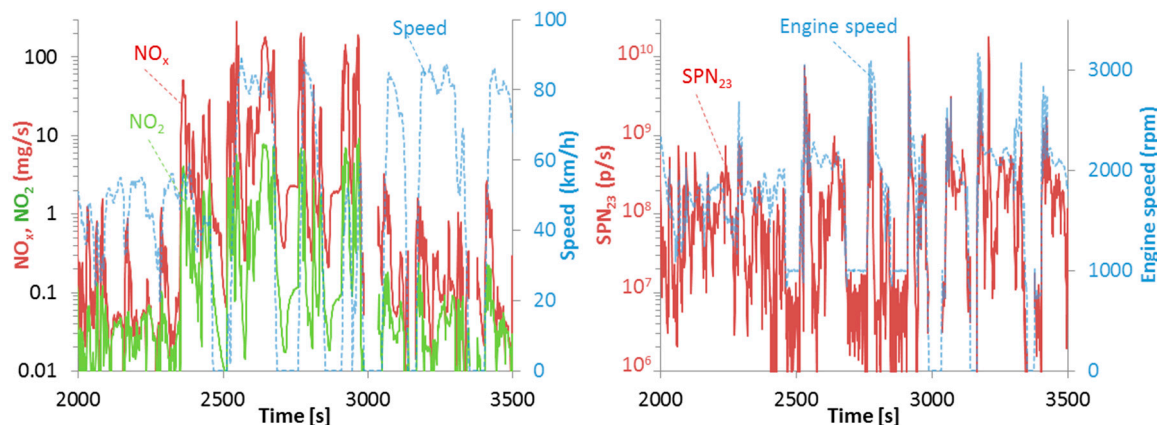

Figure 5. Solid particle number >23 nm (SPN_{23}) emissions for the motorway parts of dynamic RDE-1 (RDE-1-D) (left panel) and (normal) RDE-1 (right panel).

One of the three dynamic tests needs to be separately discussed (RDE-1D*). All emissions were higher in RDE-1D* than in the other dynamic tests on the same route (RDE-1D) or a different route (RDE-2D). The CO emissions reached almost 2500 mg/km and the NO_x exceeded 200 mg/km. High NO_x emissions took place at the end of the urban part and mainly during the rural share (see Figure 6, left panel). There is no clear explanation for this behaviour. The speed and dynamics of the specific test cannot explain the high emissions. The dynamics of this test, in terms of 95th percentile of $v \times a$, were lower than those of the other dynamic tests performed, for whole test as well as for the urban and rural share of operation (see Figure A1 of the Appendix A). Still, NO_x emissions reached extremely high concentrations (>3000 ppm), higher than those measured during cold start (<1000 ppm) where most gasoline cars present their highest NO_x emissions because the TWC has not reached its light-off temperature. The complete cycle is plotted in Figure A3 (Appendix A).

There was no clear evidence of an active GPF regeneration, as SPN_{23} emissions during this event did not vary significantly (see Figure 6, right panel). However, due to the high NO_2 emissions during the event (>100 ppm) it could be that a passive regeneration occurred at low exhaust gas temperatures. The SPN_{23} were slightly higher after the event. It is possible that the GPF was not loaded with a large amount of soot but the control unit of the vehicle misinterpreted the pressure drop due to the high accelerations as loaded filter. This was the only test where such high NO_x emissions were recorded during the entire on-road and laboratory campaign. Although there was no warning or error indication on the dashboard, we did not check the OBD for possible errors. Therefore, further studies will be needed to understand the causes of these high NO_x emissions. If the high NO_x is related to the regeneration strategy of the vehicle, the contribution of additional NO_x can be estimated by adding the emissions of the high NO_x trip weighted for the occurrence frequency. In our case the car was driven >800 km on the road, thus the contribution to the normal RDE (or WLTP) would be (maximum) another 20 mg/km (= 77/800 × 205) or 13 mg/km if the tests in the laboratory are also considered.

Figure 6. NO_x and NO_2 emissions (left panel) and solid particle number >23 nm (SPN_{23}) emissions (right panel) for the first dynamic route (RDE-1-D*).

3. Materials and Methods

The testing of this vehicle was part of four projects:

- Emissions compliance assessment.
- Assessment of vehicle emissions beyond boundary conditions of RDE.
- Development of Type VI (low temperature) test procedures.
- Monitoring of sub-23 nm emissions and evaluation of testing instrumentation.

The "sub-23 nm" project supports the discussions at the PMP (Particle Measurement Programme) meetings in order to extend the current SPN regulated methodology to a lower size (10 nm). The evaluations so far were based on GDI vehicles without GPF, so it was necessary to assess the

methodology for a GPF-equipped GDI vehicle. The "low temperature" project supports the GRPE discussions on developing a methodology to assess vehicle emissions at cold ambient temperature, −7 °C. Assessing the current draft procedures with a gasoline vehicle, which is more challenging regarding condensation, was necessary. Furthermore, evaluation of the performance of a GPF-equipped vehicle using the WLTC at cold ambient temperature was of great importance since there are not many studies in this area. The "beyond RDE boundary conditions" project aims at understanding the behaviour of vehicles at conditions that are close and beyond the boundary conditions of the current RDE procedures. This is necessary in order to better understand the implications on the environmental performance of vehicles meeting EU RDE requirements and to explore engine operations not covered within the RDE requirements. This also allows the evaluation of the emissions under conditions that may be allowed in other regions.

3.1. Vehicle and Fuel

The vehicle was a Euro 6b compliant 1.4 L gasoline vehicle equipped with a three-way catalytic converter (TWC) and an uncoated GPF (Table 3). All the tests were performed with market E5 fuel and using the default driving mode.

Table 3. Vehicle general features.

Combustion type	Spark ignition
Fuel system	Direct injection
Aftertreatment	TWC + GPF
Engine displacement (cm^3)	1395
Engine power (kW)	110
Transmission/Gearbox	Manual/6
Vehicle mass (kg)	1495
Declared CO_2 (NEDC) (g/km)	132
EU emission standard	Euro 6b
Registration year	01/2018
Mileage (km)	4950

TWC = three-way catalyst; GPF = gasoline particulate filter.

3.2. Laboratory Tests

3.2.1. Instrumentation

Laboratory emission tests were performed at JRC's (Joint Research Centre) vehicle emissions laboratory (VELA 2). The characteristics of the climatic test cell are described elsewhere [7,53]. In brief, samples were taken from the tailpipe and the diluted gas in the full dilution tunnel in real time and at the end of the test from bags that were filled during the test, as described in the regulation [54,55]. Regulated gaseous emissions were analysed by sampling diluted exhaust from a set of Tedlar bags using an integrated setup that includes non-dispersive infrared (for CO and CO_2), a chemiluminescence detector (for NO_x) and a heated (191 °C) flame ionization detector (for THC).

The solid particle number emissions (SPN) were measured from the full dilution tunnel with constant volume sampling (CVS) with an AVL (Graz, Austria) particle counter (APC 489) compliant with regulation 2017/1151 [56]. In APC, solid particles are counted downstream of a thermal pre-treatment unit with a condensational particle counter (CPC 3790, TSI Inc.) having a counting efficiency of 50% at 23 nm diameter particles, SPN_{23}. In addition, a CPC with 50% counting efficiency at 10 nm (CPC 3792, TSI Inc.) was used to determine SPN_{10}. The 10 nm CPC was sampling from APC's secondary dilution exhaust outlet.

The tests at −7 °C were conducted in a different laboratory (VELA 8) with gas analysers from AVL (Graz, Austria), series AMA i60. In this laboratory, additionally NH_3, N_2O, formaldehyde (HCHO), acetaldehyde (CH_3CHO) and aromatic compounds (AHC) emissions were monitored from the raw

exhaust using a Fourier transform infrared spectrometer (FTIR-Sesam i60 from AVL) equipped with a heated polytetrafluoroethylene sampling line at 191 °C. The FTIR instrument (Nicolet Antaris IGS Analyser-Thermo Electron Scientific Instruments LLC, Madison, WI, USA) was equipped with a multipath gas cell of 2 m of optical path, a downstream sampling pump (6.5 lpm flowrate) and had the acquisition frequency of 1 Hz with a working pressure of 860 hPa.

In order to confirm the equivalency of the laboratories, two cold start cycles at 23 °C (WLTP, Worldwide Harmonized Light Vehicles Test Procedure) were also repeated. The average of all tests in both laboratories with their variability were reported and plotted.

3.2.2. Test Cycles and Procedures

The tests were the New European Driving Cycle (NEDC) and Worldwide Harmonized Light Vehicles Test Procedure (WLTP) with cold engine start, i.e., the lubricant oil temperature was within 1 °C from the ambient temperature at the start of the cycles (25 °C for NEDC and 23 °C for WLTP). The WLTP, in addition to the new test cycle, respected all provisions from regulation 2017/1151 such as gear shift calculation, increased vehicle test mass, etc. [57]. Road loads applied on the chassis dynamometer on the NEDC and WLTP tests were calculated based on the vehicle characteristics (inertia and dimensions) applying an in-house approach that considers procedural differences between NEDC and WLTP procedures [58].

The modified tests in this study (Table 4) included hot start NEDC and WLTP, where the engine lubricant oil temperature was >70 °C [59]. Additionally, a hot NEDC immediately after a cold start NEDC (without turning off the engine) is abbreviated as "NEDC hot R". At the "NEDC hot R" tests the lubricant oil temperature at the start of the cycle was >85 °C. The vehicle emissions were also measured for cold start NEDC driven with auxiliaries on (NEDC-aux); in this study the auxiliaries were air conditioning (set at 19 °C) and lights on. All the tests were repeated two times.

Table 4. Laboratory cycles characteristics.

	NEDC	NEDC Hot	NEDC Hot R	NEDC Aux	WLTP	WLTP Hot
Dyno inertia	1470	1470	1470	1470	1704	1704
Distance (km)	10.9	10.9	10.9	10.9	23.2	23.2
Duration (min)	19.7	19.7	19.7	19.7	30	30
T_{amb} (°C)	25	25	25	25	23	23
RH (%)	50	50	50	50	50	50
Mean speed (km/h)	33.3	33.3	33.3	33.3	46.5	46.5
95th $v \times a$ (m^2/s^3)	7.5	7.5	7.5	7.5	12.5	12.5
T_{oil} (°C)	25	70	85	25	23	70

3.3. On-Road Tests

3.3.1. Instrumentation

The portable emissions measurement system (PEMS) used, an AVL MOVE system (AVL, Graz, Austria, model 2016), measured NO_x (NO and NO_2), CO, SPN_{23} and CO_2 during the on-road tests and real traffic conditions in the surroundings of the JRC site. This PEMS consists of a tailpipe attachment, heated exhaust lines, an exhaust flow meter (EFM), exhaust gas analysers, a solid particle counter, data logger connected to vehicle network, a GPS and a weather station for ambient temperature and humidity measurements. The PEMS acquired some basic engine parameters from the OBD (on-board diagnostics) port. The main PEMS unit was mounted on a trailer hook. The system measures at exhaust gas concentrations of CO and CO_2 using a non-dispersive infrared sensor and NO and NO_2 using a non-dispersive ultra-violet sensor (with two separate chemical cells for NO and NO_2). SPN_{23} was measured by means of diffusion charge methodology. The EFM uses a Pitot tube (2 inches for our tests) to calculate flow rate. The maximum measured exhaust flow rate was 382 kg/h, which corresponds to 66% of the maximum range of the flow meter. All relevant emissions data were recorded at a frequency

of 10 Hz and reported at a frequency of 1 Hz. The instrument uncertainty is expected in the order of 20% for CO [60], 40% for NO_x [61] and 60% for particle number [62].

3.3.2. Routes

On the road, tests were performed within and outside the boundary conditions of the RDE regulation. Table 5 summarizes the main characteristics of the four routes used. The vehicle was driven on two routes (RDE-1 and Route RDE-2) designed to meet all the criteria from the RDE regulation (trip duration, composition, temperature range, altitude range, cumulative positive elevation gain, etc.). Details on the routes can be found elsewhere [7]. The vehicle was additionally tested on both routes but driven with a more aggressive driving style (RDE-1-D and RDE-2-D), resulting in more dynamic trip indicators (closer to or above max. 95th percentile of $v \times a$ RDE limits, see Figure A1 in the Appendix A). The higher dynamics were achieved, for example, by faster starts after fully stopping the vehicle at traffic lights or engaging lower gears when using manual transmission. RDE-1 was additionally driven in a dynamic way by another driver (RDE-1-D*). All tests were performed respecting the Italian traffic code. Additionally, another two non-RDE compliant routes that represent prolonged motorway drive (City-Motor) and hilly driving (Hill) were used. PEMS testing was performed on public paved roads, with little to no congestion. Ambient temperature during the test campaign ranged from 20 °C to 28 °C, similar to the laboratory test temperatures. One repetition per test was performed.

Table 5. On-road routes characteristics.

	RDE-1	RDE-2	RDE-1-D	RDE-1-D *	RDE-2-D	City-Motor	Hill
Distance (km)	78	94	78	77	93	139	62
Duration (min)	99	112	94	96	104	136	106
Mean T_{amb} (°C)	22	23	20	28	23	26	23
RH (%)	67	69	75	34	63	57	67
Urban stop time (%)	22	20	25	25	21	14	8
Urban distance (km)	31	37	29	28	33	40	62
Rural distance (km)	25	26	26	26	29	18	-
Motorway distance (km)	22	31	23	23	31	81	-
Mean eng. speed (rpm)	1400	1515	1810	1730	1815	1730	1330
Mean speed (km/h)	48.0	50.5	50.3	49.0	54.2	61.3	34.5
Urban 95th $v \times a$ (m^2/s^3)	10.7	11.4	20.7	15.6	20.3	10.8	8.8
Rural 95th $v \times a$ (m^2/s^3)	16.6	15.4	29.6	26.0	28.9	17.2	-
Motor. 95th $v \times a$ (m^2/s^3)	14.8	16.1	31.5	23.4	31.5	17.9	-
CPEG (m/100 km)	800	878	760	760	820	440	1830
Max altitude	300	410	300	300	410	300	1100

CPEG = cumulative positive elevation gain.

3.4. Calculations

The laboratory results were the given by the chassis dynamometer automation software. Especially for particles, the dilution and the particle losses were taken into account according to the regulation with the average particle number concentration reduction factor (PCRF) of 30, 50 and 100 nm. The loss correction for the sub-23 nm particle emission is made using the equation [63]:

$$SPN_{10} = SPN_{10,uncor} + PCRF_{15} \times (SPN_{10} - SPN_{23}), \tag{1}$$

where $SPN_{10,uncor}$ and SPN_{23} are the emissions calculated with the set $PCRF_{30\text{-}50\text{-}100}$ value (in APC), $PCRF_{15}$ is the correction coefficient and SPN_{10} is the corrected particle emission. The 15 nm PCRF was selected for sub-23 nm particle loss correction as the diameter is about the same as the geometric mean of 10 nm and 23 nm and it represents an average PCRF in sub-23 nm measurement size range. The $PCRF_{15}$ was determined with thermally pre-treated, diffusion-flame generated monodisperse particles at the external sampling position and was found to exceed the set PCRF value by 70%, thus the $PCRF_{15}$ was 1.7.

The on-road emissions were calculated by integrating the total mass emissions measured during the test and dividing the obtained value by the driven distance, as estimated from the GPS velocity signal using EMROAD version 6.01, the ad-hoc tool developed in-house. These are the so-called 'raw integrated' emissions (without using the weighting function based on CO_2 emissions as introduced in the fourth package of the RDE regulation EU 2018/1832). All the emissions including cold-start and idle emissions along the test have been included in the data analysis as required by the third (regulation EU 2017/1154) and the forth (latest) package of the RDE regulation EU 2018/1832. No correction for extended altitude (>700 m) and extended temperature (>30 °C) conditions were applied. The verification of the overall trip dynamics was done using the moving averaging window method, as prescribed in EU regulation 2018/1832, and using the average distance-specific WLTP CO_2 of the Type I tests performed in the two laboratories.

4. Conclusions

In this study we investigated one of the first vehicles with a gasoline particulate filter (GPF) in mass production available in the European market. The studies so far were based mainly on retrofitted or prototype vehicles, thus, our results set a basis for future studies with commercial GPF-equipped vehicles. The evaluation included laboratory tests with various test cycles at different temperatures and modified parameters. Both regulated and non-regulated pollutants were measured. In addition to current regulation compliant test cycles and RDE tests, on-road tests at high altitude and dynamic driving conditions were conducted, covering a wider engine map.

The results showed that the vehicle fulfilled all applicable limits in the laboratory. Solid particle number emissions (SPN) were more than 10 times lower than the current limit, NO_x half of the limit and CO was one fifth. The excess of SPN_{10} in comparison to SPN_{23} was approximately 20–50%, including the modified cycles. Yet, similarly to SPN_{23}, SPN_{10} emissions were also below 10% of the current PN limit of 6×10^{11} p/km. The majority of particles were emitted during the cold engine start. The NO_2 to NO_x ratio reached 50% in the laboratory tests. The ammonia was 11 mg/km and the other non-regulated pollutants such as formaldehyde and acetaldehyde were negligible. The tests at −7 °C increased the emissions, but they stayed within the regulated 23 °C limits for CO, NO_x and SPN. At cold temperature, the total hydrocarbons and non-methane hydrocarbons exceeded the 23 °C limits by 29% and 74% respectively. Ammonia reached 27 mg/km. Modifications of the type approval test conditions gave similar results.

The on-road tests results were similar to the laboratory. For the various routes tested, which included RDE compliant routes, a high motorway share route and a hilly route, NO_x emissions were around 15–25 mg/km (NO_2 to NO_x 10%), CO 133–189 mg/km and SPN $1.3–2 \times 10^{10}$ p/km. The CO_2 emissions were approximately 30% higher than the type approval value at the RDE compliant routes. Dynamic driving doubled the SPN emissions, although they remained very low, but increased CO up to 20 times. For only one test and during the rural part, NO_x emissions increased significantly. The results of this study confirmed the effectiveness of GPFs in controlling particle emissions under all driving and boundary conditions. Further studies with GPF-equipped commercial vehicles to better understand their performance during regenerations and over their lifetime are needed.

Disclaimer: The opinions expressed in this manuscript are those of the authors and should in no way be considered to represent an official opinion of the European Commission. Mention of trade names or commercial products does not constitute endorsement or recommendation by the authors or the European Commission.

Appendix A

The dynamics (as velocity per acceleration) of the on-road tests is plotted in Figure A1. For all the on-road tests, instantaneous vehicle speed was split in three bins representing Urban (≤60 km/h), Rural (>60 km/h and ≤90 km/h) and Motorway (>90 km/h) driving conditions. For the laboratory tests (NEDC and WLTC) the evaluation was done for each phase.
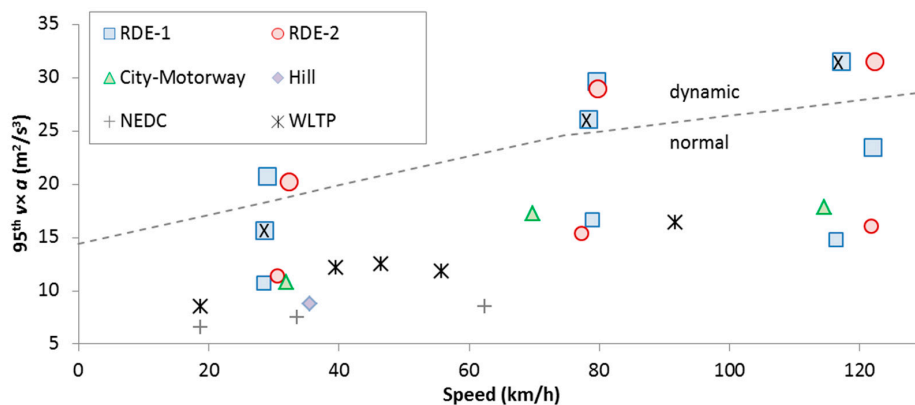

Figure A1. Summary of the dynamics, in terms of 95th percentile of $v \times a$ for the laboratory and RDE routes. The "x" in the square symbols indicate the RDE-1-D* route driven by a different driven. Dotted line indicates the 95th percentile of $v \times a$ boundary. Dynamic tests have bigger symbols. The laboratory cycles are divided into their respective parts. Note that Hill route only has an urban section. RDE = real-driving emissions; NEDC = New European Driving Cycle; WLTP = Worldwide Harmonised Light Vehicles Test Procedure.

Real time emission rates for various pollutants can be seen in Figures A2 and A3.
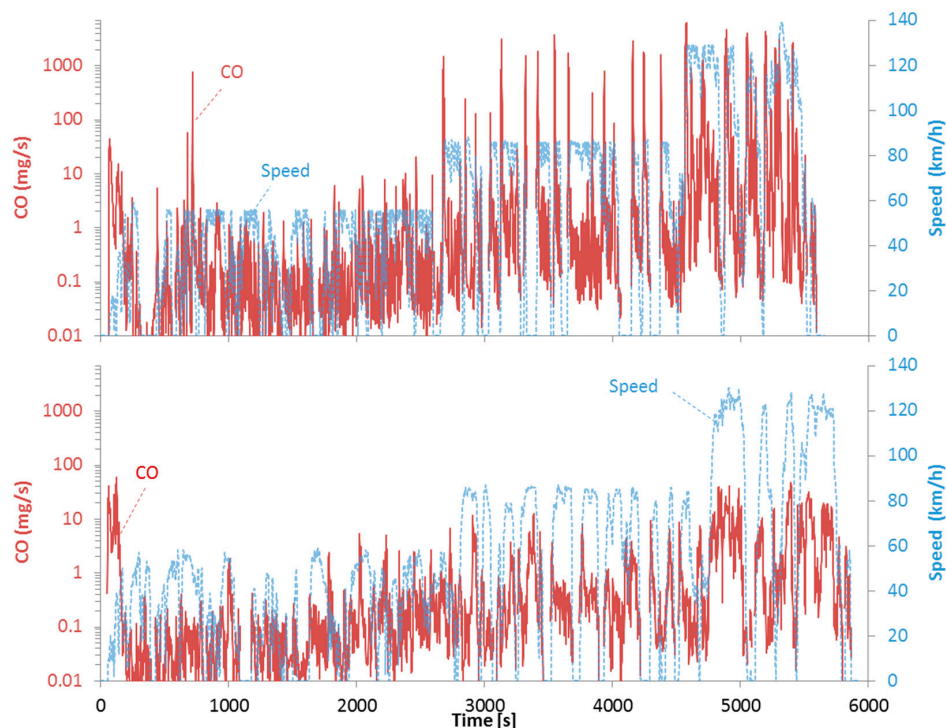
Figure A2. Carbon monoxide (CO) emissions for (normal) RDE-1 (lower panel) and dynamic RDE-1 (RDE-1-D) (upper panel).
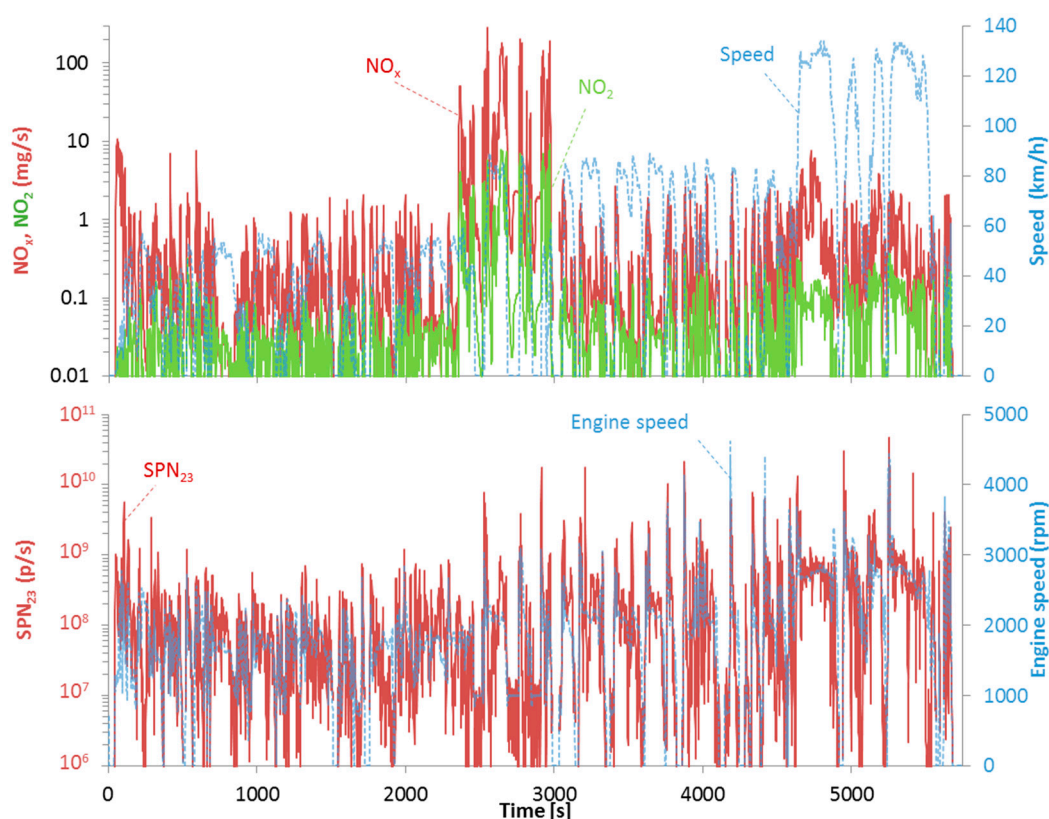
Figure A3. NO_x and NO_2 emissions (upper panel) and solid particle number >23 nm (SPN_{23}) emissions (lower panel) for RDE-1-D*.

References

1. Giechaskiel, B.; Mamakos, A.; Andersson, J.; Dilara, P.; Martini, G.; Schindler, W.; Bergmann, A. Measurement of automotive nonvolatile particle number emissions within the European legislative framework: A review. *Aerosol. Sci. Technol.* **2012**, *46*, 719–749. [CrossRef]

2. Giechaskiel, B.; Joshi, A.; Ntziachristos, L.; Dilara, P. European regulatory framework and particulate matter emissions of gasoline light-duty vehicles: A review. *Catalysts* **2019**, *9*, 586. [CrossRef]

3. Müller, J.-O.; Frank, B.; Jentoft, R.E.; Schlögl, R.; Su, D.S. The oxidation of soot particulate in the presence of NO2. *Catal. Today* **2012**, *191*, 106–111. [CrossRef]

4. Quiros, D.C.; Hu, S.; Hu, S.; Lee, E.S.; Sardar, S.; Wang, X.; Olfert, J.S.; Jung, H.S.; Zhu, Y.; Huai, T. Particle effective density and mass during steady-state operation of GDI, PFI, and diesel passenger cars. *J. Aerosol. Sci.* **2015**, *83*, 39–54. [CrossRef]

5. Wang, C.; Xu, H.; Herreros, J.M.; Lattimore, T.; Shuai, S. Fuel effect on particulate matter composition and soot oxidation in a direct-injection spark ignition (DISI) engine. *Energy Fuels* **2014**, *28*, 2003–2012. [CrossRef]

6. Choi, S.; Seong, H. Oxidation characteristics of gasoline direct-injection (GDI) engine soot: Catalytic effects of ash and modified kinetic correlation. *Combust. Flame* **2015**, *162*, 2371–2389. [CrossRef]

7. Clairotte, M.; Valverde, V.; Bonnel, P.; Giechaskiel, P.; Carriero, M.; Otura, M.; Fontaras, G.; Pavlovic, J.; Martini, G.; Krasenbrink, A. *Joint Research Centre 2017 Light-Duty Vehicles Emissions Testing Contribution to the EU Market Surveillance: Testing Protocols and Vehicle Emissions Performance*; Publications Office of the European Union: Luxembourg, 2018; ISBN 978-92-79-90600-8.

8. Valverde, V.; Mora, B.A.; Clairotte, M.; Pavlovic, J.; Suarez-Bertoa, R.; Giechaskiel, B.; Astorga-LLorens, C.; Fontaras, G. Emission factors derived from 13 Euro 6b light-duty vehicles based on laboratory and on-road measurements. *Atmosphere* **2019**, *10*, 243. [CrossRef]

9. Suarez-Bertoa, R.; Valverde-Morales, V.; Clairotte, M.; Pavlovic, J.; Giechaskiel, B.; Franco, V.; Kregar, Z.; Astorga-LLorens, C. On-road emissions of passenger cars beyond the boundary conditions of the real-driving emissions test. *Environ. Res.* **2019**, *176*, 108572. [CrossRef]

10.   Guerreiro, C.; González Ortiz, A.; Leeuw, F.; de Viana, M.; Colette, A. *European Environment Agency Air Quality in Europe—2018 Report*; Publications Office of the European Union: Luxembourg, 2018; ISBN 978-92-9213-989-6.

11.   Suarez-Bertoa, R.; Mendoza-Villafuerte, P.; Riccobono, F.; Vojtisek, M.; Pechout, M.; Perujo, A.; Astorga, C. On-road measurement of NH3 emissions from gasoline and diesel passenger cars during real world driving conditions. *Atmos. Environ.* **2017**, *166*, 488–497. [CrossRef]

12.   Park, G.; Mun, S.; Hong, H.; Chung, T.; Jung, S.; Kim, S.; Seo, S.; Kim, J.; Lee, J.; Kim, K.; et al. Characterization of emission factors concerning gasoline, LPG, and diesel vehicles via transient chassis-dynamometer tests. *Appl. Sci.* **2019**, *9*, 1573. [CrossRef]

13.   Barbier, J.; Duprez, D. Steam effects in three-way catalysis. *Appl. Catal. B Environ.* **1994**, *4*, 105–140. [CrossRef]

14.   Bradow, R.L.; Stump, F.D. *Unregulated Emissions from Three-Way Catalyst Cars*; No. 770369; SAE: Warrendale, PA, USA, 1977; p. 0369.

15.   Bishop, G.A.; Peddle, A.M.; Stedman, D.H.; Zhan, T. On-road emission measurements of reactive nitrogen compounds from three California cities. *Environ. Sci. Technol.* **2010**, *44*, 3616–3620. [CrossRef] [PubMed]

16.   Schuetzle, D.; Siegl, W.O.; Jensen, T.E.; Dearth, M.A.; Kaiser, E.W.; Gorse, R.; Kreucher, W.; Kulik, E. The relationship between gasoline composition and vehicle hydrocarbon emissions: A review of current studies and future research needs. *Environ. Health Perspect.* **1994**, *102*, 3–12. [PubMed]

17.   Zervas, E.; Montagne, X.; Lahaye, J. Emission of alcohols and carbonyl compounds from a spark ignition engine. influence of fuel and air/fuel equivalence ratio. *Environ. Sci. Technol.* **2002**, *36*, 2414–2421. [CrossRef] [PubMed]

18.   Muñoz, M.; Haag, R.; Zeyer, K.; Mohn, J.; Comte, P.; Czerwinski, J.; Heeb, N.V. Effects of four prototype gasoline particle filters (GPFs) on nanoparticle and genotoxic PAH emissions of a gasoline direct injection (GDI) vehicle. *Environ. Sci. Technol.* **2018**, *52*, 10709–10718. [CrossRef] [PubMed]

19.   Joshi, A.; Johnson, T. Gasoline particulate filters—A review. *Emiss. Control Sci. Technol.* **2018**, *4*, 219–239. [CrossRef]

20.   Suarez-Bertoa, R.; Astorga, C. Impact of cold temperature on Euro 6 passenger car emissions. *Environ. Pollut.* **2018**, *234*, 318–329. [CrossRef]

21.   Rodriguez, F.; Dornoff, J. *Beyond NOx: Emissions of Unregulated Pollutants from a Modern Gasoline Car*; The International Council on Clean Transportation (ICCT): Berlin, Germany, 2019.

22.   Demuynck, J.; Favre, C.; Bosteels, D.; Hamje, H.; Andersson, J. *Real-World Emissions Measurements of a Gasoline Direct Injection Vehicle without and with a Gasoline Particulate Filter*; No. 2017-01-0985; SAE: Warrendale, PA, USA, 2017.

23.   Ito, Y.; Shimoda, T.; Aoki, T.; Yuuki, K.; Sakamoto, H.; Kato, K.; Thier, D.; Kattouah, P.; Ohara, E.; Vogt, C. *Next Generation of Ceramic Wall Flow Gasoline Particulate Filter with Integrated Three Way Catalyst*; No. 2015-01-1073; SAE: Warrendale, PA, USA, 2015.

24.   Richter, J.M.; Klingmann, R.; Spiess, S.; Wong, K.-F. Application of catalyzed gasoline particulate filters to GDI vehicles. *SAE Int. J. Engines* **2012**, *5*, 1361–1370. [CrossRef]

25.   Wang, X.; Ge, Y.; Gong, H.; Yang, Z.; Tan, J.; Hao, L.; Su, S. Ammonia emissions from China-6 compliant gasoline vehicles tested over the WLTC. *Atmos. Environ.* **2019**, *199*, 136–142. [CrossRef]

26.   Choi, K.; Kim, J.; Ko, A.; Myung, C.-L.; Park, S.; Lee, J. Size-resolved engine exhaust aerosol characteristics in a metal foam particulate filter for GDI light-duty vehicle. *J. Aerosol. Sci.* **2013**, *57*, 1–13. [CrossRef]

27.   Pieber, S.M.; Kumar, N.K.; Klein, F.; Comte, P.; Bhattu, D.; Dommen, J.; Bruns, E.A.; Kılıç, D.; El Haddad, I.; Keller, A.; et al. Gas-phase composition and secondary organic aerosol formation from standard and particle filter-retrofitted gasoline direct injection vehicles investigated in a batch and flow reactor. *Atmos. Chem. Phys.* **2018**, *18*, 9929–9954. [CrossRef]

28.   Guan, B.; Zhan, R.; Lin, H.; Huang, Z. Review of state of the art technologies of selective catalytic reduction of NOx from diesel engine exhaust. *Appl. Therm. Eng.* **2014**, *66*, 395–414. [CrossRef]

29.   Suarez-Bertoa, R.; Astorga, C. Isocyanic acid and ammonia in vehicle emissions. *Transp. Res. Part D Transp. Environ.* **2016**, *49*, 259–270. [CrossRef]

30.   Bielaczyc, P.; Woodburn, J.; Szczotka, A. *Investigations into Particulate Emissions from EURO 5 Passenger Cars with DISI Engines Tested at Multiple Ambient Temperatures*; No. 2015-24-2517; SAE: Warrendale, PA, USA, 2015.

31. Suarez-Bertoa, R.; Pavlovic, J.; Trentadue, G.; Otura-Garcia, M.; Tansini, A.; Ciuffo, B.; Astorga, C. Effect of low ambient temperature on emissions and electric range of plug-in hybrid electric vehicles. *ACS Omega* **2019**, *4*, 3159–3168. [CrossRef]

32. Jang, J.; Lee, J.; Choi, Y.; Park, S. Reduction of particle emissions from gasoline vehicles with direct fuel injection systems using a gasoline particulate filter. *Sci. Total Environ.* **2018**, *644*, 1418–1428. [CrossRef]

33. Suarez-Bertoa, R.; Zardini, A.A.; Keuken, H.; Astorga, C. Impact of ethanol containing gasoline blends on emissions from a flex-fuel vehicle tested over the Worldwide Harmonized Light duty Test Cycle (WLTC). *Fuel* **2015**, *143*, 173–182. [CrossRef]

34. Clairotte, M.; Adam, T.W.; Zardini, A.A.; Manfredi, U.; Martini, G.; Krasenbrink, A.; Vicet, A.; Tournié, E.; Astorga, C. Effects of low temperature on the cold start gaseous emissions from light duty vehicles fuelled by ethanol-blended gasoline. *Appl. Energy* **2013**, *102*, 44–54. [CrossRef]

35. Suarez-Bertoa, R.; Clairotte, M.; Arlitt, B.; Nakatani, S.; Hill, L.; Winkler, K.; Kaarsberg, C.; Knauf, T.; Zijlmans, R.; Boertien, H.; et al. Intercomparison of ethanol, formaldehyde and acetaldehyde measurements from a flex-fuel vehicle exhaust during the WLTC. *Fuel* **2017**, *203*, 330–340. [CrossRef]

36. Suarez-Bertoa, R.; Astorga, C. Unregulated emissions from light-duty hybrid electric vehicles. *Atmos. Environ.* **2016**, *136*, 134–143. [CrossRef]

37. Bielaczyc, P.; Woodburn, J.; Szczotka, A. Low ambient temperature cold start emissions of gaseous and solid pollutants from Euro 5 vehicles featuring direct and indirect injection spark-ignition engines. *SAE Int. J. Fuels Lubr.* **2013**, *6*, 968–976. [CrossRef]

38. Weber, C.; Sundvor, I.; Figenbaum, E. Comparison of regulated emission factors of Euro 6 LDV in Nordic temperatures and cold start conditions: Diesel- and gasoline direct-injection. *Atmos. Environ.* **2019**, *206*, 208–217. [CrossRef]

39. Zhu, R.; Hu, J.; Bao, X.; He, L.; Lai, Y.; Zu, L.; Li, Y.; Su, S. Tailpipe emissions from gasoline direct injection (GDI) and port fuel injection (PFI) vehicles at both low and high ambient temperatures. *Environ. Pollut.* **2016**, *216*, 223–234. [CrossRef] [PubMed]

40. Weilenmann, M.; Soltic, P.; Saxer, C.; Forss, A.-M.; Heeb, N. Regulated and nonregulated diesel and gasoline cold start emissions at different temperatures. *Atmos. Environ.* **2005**, *39*, 2433–2441. [CrossRef]

41. Weilenmann, M.; Favez, J.-Y.; Alvarez, R. Cold-start emissions of modern passenger cars at different low ambient temperatures and their evolution over vehicle legislation categories. *Atmos. Environ.* **2009**, *43*, 2419–2429. [CrossRef]

42. Fontaras, G.; Ciuffo, B.; Zacharof, N.; Tsiakmakis, S.; Marotta, A.; Pavlovic, J.; Anagnostopoulos, K. The difference between reported and real-world CO2 emissions: How much improvement can be expected by WLTP introduction? *Transp. Res. Procedia* **2017**, *25*, 3933–3943. [CrossRef]

43. Mamakos, A.; Martini, G.; Marotta, A.; Manfredi, U. Assessment of different technical options in reducing particle emissions from gasoline direct injection vehicles. *J. Aerosol. Sci.* **2013**, *63*, 115–125. [CrossRef]

44. Ito, Y.; Shimoda, T.; Aoki, T.; Shibagaki, Y.; Yuuki, K.; Sakamoto, H.; Vogt, C.; Matsumoto, T.; Heuss, W.; Kattouah, P. *Advanced Ceramic Wall Flow Filter for Reduction of Particulate Number Emission of Direct Injection Gasoline Engines*; No. 2013-01-0836; SAE: Warrendale, PA, USA, 2013.

45. Zhang, R.; Howard, K.; Kirkman, P.; Browne, D.; Lu, Z.; He, S.; Boger, T. *A Study into the Impact of Engine Oil on Gasoline Particulate Filter Performance Through a Real-World Fleet Test*; No. 2019-01-0299; SAE: Warrendale, PA, USA, 2019.

46. Chan, T.W.; Saffaripour, M.; Liu, F.; Hendren, J.; Thomson, K.A.; Kubsh, J.; Brezny, R.; Rideout, G. Characterization of real-time particle emissions from a gasoline direct injection vehicle equipped with a catalyzed gasoline particulate filter during filter regeneration. *Emiss. Control Sci. Technol.* **2016**, *2*, 75–88. [CrossRef]

47. Giechaskiel, B.; Lähde, T.; Suarez-Bertoa, R.; Clairotte, M.; Grigoratos, T.; Zardini, A.; Perujo, A.; Martini, G. Particle number measurements in the European legislation and future JRC activities. *Combust. Engines* **2018**, *174*, 3–16.

48. Giechaskiel, B.; Manfredi, U.; Martini, G. Engine exhaust solid sub-23 nm particles: I. literature survey. *SAE Int. J. Fuels Lubr.* **2014**, *7*, 950–964. [CrossRef]

49. Giechaskiel, B.; Vanhanen, J.; Väkevä, M.; Martini, G. Investigation of vehicle exhaust sub-23 nm particle emissions. *Aerosol. Sci. Technol.* **2017**, *51*, 626–641. [CrossRef]

50. Yamada, H.; Inomata, S.; Tanimoto, H. Particle and VOC emissions from stoichiometric gasoline direct injection vehicles and correlation between particle number and mass emissions. *Emiss. Control Sci. Technol.* **2017**, *3*, 135–141. [CrossRef]

51. Saffaripour, M.; Chan, T.W.; Liu, F.; Thomson, K.A.; Smallwood, G.J.; Kubsh, J.; Brezny, R. Effect of drive cycle and gasoline particulate filter on the size and morphology of soot particles emitted from a gasoline-direct-injection vehicle. *Environ. Sci. Technol.* **2015**, *49*, 11950–11958. [CrossRef] [PubMed]

52. Yamada, H.; Funato, K.; Sakurai, H. Application of the PMP methodology to the measurement of sub-23 nm solid particles: Calibration procedures, experimental uncertainties, and data correction methods. *J. Aerosol. Sci.* **2015**, *88*, 58–71. [CrossRef]

53. Giechaskiel, B.; Suarez-Bertoa, R.; Lahde, T.; Clairotte, M.; Carriero, M.; Bonnel, P.; Maggiore, M. Emissions of a Euro 6b Diesel Passenger Car Retrofitted with a Solid Ammonia Reduction System. *Atmosphere* **2019**, *10*, 180. [CrossRef]

54. Adachi, M.; Nakamura, H. (Eds.) *Engine Emissions Measurement Handbook: HORIBA Automotive Test Systems*; SAE International: Warrendale, PA, USA, 2014; ISBN 978-0-7680-8012-4.

55. Varella, R.; Giechaskiel, B.; Sousa, L.; Duarte, G. Comparison of Portable Emissions Measurement Systems (PEMS) with Laboratory Grade Equipment. *Appl. Sci.* **2018**, *8*, 1633. [CrossRef]

56. Giechaskiel, B.; Cresnoverh, M.; Jörgl, H.; Bergmann, A. Calibration and accuracy of a particle number measurement system. *Meas. Sci. Technol.* **2010**, *21*, 045102. [CrossRef]

57. Pavlovic, J.; Ciuffo, B.; Fontaras, G.; Valverde, V.; Marotta, A. How much difference in type-approval CO_2 emissions from passenger cars in Europe can be expected from changing to the new test procedure (NEDC vs. WLTP)? *Transp. Res. Part A Policy Pract.* **2018**, *111*, 136–147. [CrossRef]

58. Tsiakmakis, S.; Fontaras, G.; Ciuffo, B.; Samaras, Z. A simulation-based methodology for quantifying European passenger car fleet CO_2 emissions. *Appl. Energy* **2017**, *199*, 447–465. [CrossRef]

59. European Commission. *Guidance on the Evaluation of Auxiliary Emission Strategies and the Presence of Defeat Devices with Regard to the Application of Regulation (EC) no 715/2007 on Type Approval of Motor Vehicles with Respect to Emissions from Light Passenger and Commercial Vehicles (Euro 5 and euro 6). Commission Notice C (2017) 352 2017*; Publications Office of the European Union: Luxembourg, 2017.

60. Giechaskiel, B.; Gioria, R.; Carriero, M.; Lähde, T.; Forloni, F.; Perujo, A.; Martini, G.; Bissi, L.M.; Terenghi, R. Emission factors of a Euro VI heavy-duty diesel refuse collection vehicle. *Sustainability* **2019**, *11*, 1067. [CrossRef]

61. Giechaskiel, B.; Clairotte, M.; Valverde-Morales, V.; Bonnel, P.; Kregar, Z.; Franco, V.; Dilara, P. Framework for the assessment of PEMS (Portable Emissions Measurement Systems) uncertainty. *Environ. Res.* **2018**, *166*, 251–260. [CrossRef]

62. Giechaskiel, B.; Schwelberger, M.; Delacroix, C.; Marchetti, M.; Feijen, M.; Prieger, K.; Andersson, S.; Karlsson, H.L. Experimental assessment of solid particle number Portable Emissions Measurement Systems (PEMS) for heavy-duty vehicles applications. *J. Aerosol Sci.* **2018**, *123*, 161–170. [CrossRef]

63. Giechaskiel, B.; Lähde, T.; Drossinos, Y. Regulating particle number measurements from the tailpipe of light-duty vehicles: The next step? *Environ. Res.* **2019**, *172*, 1–9. [CrossRef] [PubMed]